

# We are IntechOpen, the world's leading publisher of Open Access books Built by scientists, for scientists

6,900

Open access books available

185,000

International authors and editors

200M

Downloads

Our authors are among the

154

Countries delivered to

TOP 1%

most cited scientists

12.2%

Contributors from top 500 universities



WEB OF SCIENCE™

Selection of our books indexed in the Book Citation Index  
in Web of Science™ Core Collection (BKCI)

Interested in publishing with us?  
Contact [book.department@intechopen.com](mailto:book.department@intechopen.com)

Numbers displayed above are based on latest data collected.  
For more information visit [www.intechopen.com](http://www.intechopen.com)



# Development of Metal Matrix Composites Using Microwave Sintering Technique

Penchal Reddy Matli, Rana Abdul Shakoor and  
Adel Mohamed Amer Mohamed

Additional information is available at the end of the chapter

<http://dx.doi.org/10.5772/68081>

## Abstract

In this book chapter, aluminum (Al)-based metal matrix composites (AMMCs) with various reinforcing ceramic particles, such as SiC, Si<sub>3</sub>N<sub>4</sub>, and Al<sub>2</sub>O<sub>3</sub>, were produced by microwave sintering and subsequent hot extrusion processes. The role of various nano/micro-sized reinforcements in altering the structural, mechanical, and thermal properties of the microwave-extruded composites was systematically studied. The X-ray diffraction (XRD) patterns indicated that the main components were Al, SiC, Si<sub>3</sub>N<sub>4</sub>, and Al<sub>2</sub>O<sub>3</sub> for the studied Al-SiC, Al-Si<sub>3</sub>N<sub>4</sub>, and Al-Al<sub>2</sub>O<sub>3</sub> composites, respectively. Scanning electron microscopy (SEM) and energy dispersive spectroscopy (EDS) elemental mapping confirm the homogeneous distribution of reinforcing particles in the Al matrix. Mechanistic studies revealed that the Al-Si<sub>3</sub>N<sub>4</sub> metal matrix composite exhibited superior hardness, ultimate compression/tensile strength, and Young's modulus, while having a lower coefficient of thermal expansion compared to other studied Al composites. Findings presented are expected to pave the way to design, develop, and synthesize other aluminum-based metal matrix composites for automotive and industrial applications.

**Keywords:** Al matrix composites, ceramic reinforcements, microwave sintering, hot extrusion, mechanical properties, thermal properties, fracture behavior

## 1. Introduction

Microwaves occupy the portion of electromagnetic radiation spectrum between 300 MHz and 300 GHz with wavelengths ranging from 1 mm to 1 m in free space. Although the frequencies available for processing of materials are 24.124 GHz, 5.8 GHz, 2.45 GHz, and 915 MHz, generally it is carried out at 915 MHz and 2.45 GHz. Usually, 9.15 and 2.45 GHz are commonly

used in industrial equipment [1, 2]. Microwave cavities are of two types: single-mode resonance cavities and multimode resonance cavities. Single-mode cavities are specially designed and generally used for industrial applications. The domestic microwave ovens are multimode cavities in which multiple plane waves impinge on the load (material to be heated) from different directions. The microwave radiation and heating were applied to the fabrication of ceramic materials till the 1990s [3–5].

### 1.1. Characteristics and merits of microwave sintering process

Microwave sintering has attained global acceptance because of superior benefits over the traditional sintering techniques. The characteristic (**Figure 1**) of microwave heating is basically different from conventional heating [6]. For conventional heating, an external heating element is used for heat generation and then it transferred to the test materials through convention, conduction, and radiation. In microwave heating, the heat is generated internally within the test sample by rapid oscillation of dipoles at microwave frequencies [7], instead of diffusion from external sources and hence the heating is from the core of the sample to outside. Heating is very rapid and volumetric due to energy conversion rather than energy transfer as in conventional heating.

Microwave heating has many advantages over conventional heating, including cost and energy savings, and considerable reduction in processing time [8]. By using microwave energy as a heating source, short sintering time at desired temperature offers an opportunity to control, especially the microstructure coarsening during sintering, leading to excellent mechanical properties [9]. Instead of using only microwaves as a heating source, microwave heating system through a combination of conventional conduction heating and energy conversion heating using a microwave is found to be more advantageous for heating or sintering of materials [10–12]. The advantages of microwave rapid sintering include rapid and more uniform heating, prevention of hot spot formation, and more uniform and finer microstructure leading to high-performance products [13, 14].

### 1.2. Microwave sintering of materials

In principle, sintering is one of the consolidation methods to make bulk objects from loose powder compacts by heating the material below its melting point. Conventionally, the green body (unsintered powder compact) is sintered using resistant heating. Since the resistive heating is the application of thermal energy, sintering process depends on the diffusion of atoms

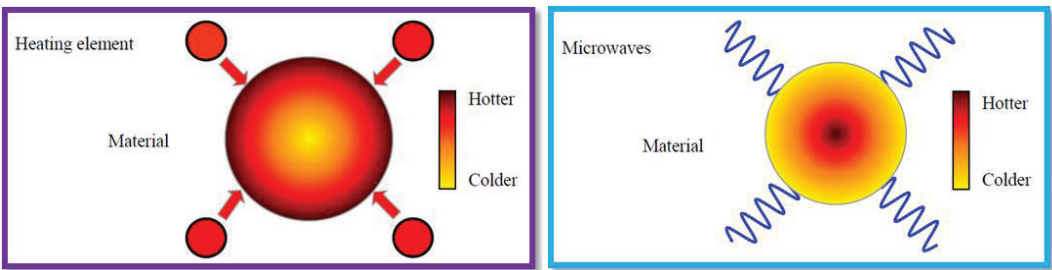


**Figure 1.** Heat distribution within a material during conventional and microwave heating.

that cause the adherence of loose particles to each other [13]. Sintering of materials using microwaves is a newly explored method, and it has been applied successfully in processing of various materials. For sintering using microwaves, the electromagnetic contrivance of the microwaves interact directly with the materials and, magnetic and dielectric losses lead to self-heating of materials. Initially, microwave energy was used to sinter various types of ceramic materials [9, 15]. By using microwave sintering, equal or superior performance ceramic products [16–18] can be produced through shorter sintering time at a lower temperature and at low cost when compared to the conventional sintered products. At room temperature, most of the ceramics do not couple well with microwaves particularly at 2.45 GHz microwave frequency and they are not heated appreciably [19]. Their coupling efficiency can be increased by increasing the temperature, using microwave susceptor/absorber, varying their morphology, and changing the microwave frequency. In most of the hybrid sintering methods, SiC of various forms such as SiC rods [4] with SiC sample holders [20] are preferably used mainly due to its high loss factor.

Most of the investigations [21–25] were conducted on the microwave sintering of semiconductors, inorganic, ceramics, and polymeric materials until 2000. Lack of research on microwave sintering of metals is based on the well-known fact that all metals reflect the microwaves causing arching during microwave heating and thus limited diffusion of the microwave waves. Later, researchers grabbed that arching phenomenon applies only for metal-based composites in the form of powder compacts [14, 26]. The idea of applying microwave energy to sinter metals and metallic materials is relatively new and limited studies on sintering of metal-based materials are available in the literature. From the literature, most of the studies are reported on the microwave sintering of iron-based materials and only a few reports are available on aluminum-, magnesium-, and copper-based materials/composites [14, 26–29].

## 2. Metal matrix composites

Development of metal matrix composites (MMCs) has been an important innovation in materials engineering over the past three decades. Metal matrix composites offer several attractive advantages over traditional engineering materials due to their superior properties [30, 31]. Metal matrix composites can be divided into three broad categories (**Figure 2**): (i) continuous fiber-reinforced matrix composites, (ii) small fiber-reinforced matrix composites, and (iii) particulate-rein-

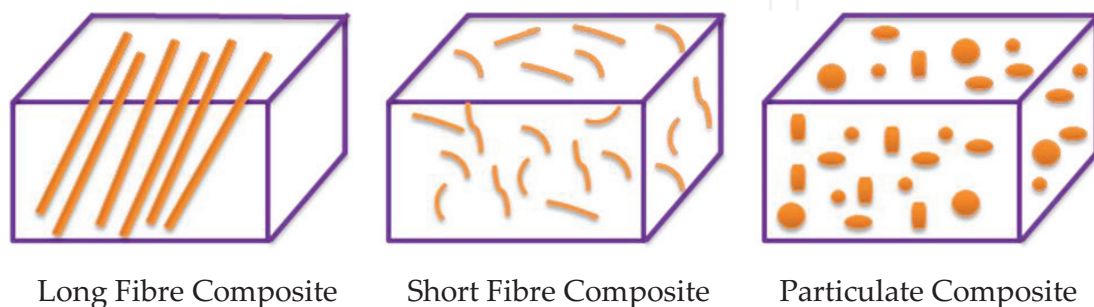


**Figure 2.** Types of reinforcement in a composite.

forced matrix composites. Among all these, particulate-reinforced metal matrix composites have gained decent interest because of their superior properties and low manufacturing expenditure. In light metal matrix composites (MMCs) [32], Al or Mg is mostly used as a base metal matrix, and ceramic particles (carbides, nitrides, and oxides) are generally used as reinforcement phase.

Nowadays, the demand of reducing energy consumption, especially in automotive industries, is becoming a critical issue. Development of lightweight aluminum-based composites can be considered as one of the promising solutions to address this issue.

The nano-sized reinforcements have a major role in improving the physical and mechanical properties which can be achieved by the addition of small volume fractions ( $\leq 2\%$ ), whereas for micron-sized particle-reinforced metal matrix composites higher volume fractions ( $\gg 10\%$ ) are essential [27]. Further addition of reinforcement will cause degradation of composite properties, which can be attributed to the possible agglomeration, clustering of reinforcement, and micro-porosity in the nanocomposites. Recently, there has been considerable interest in the production of metal matrix nanocomposites in which nanoparticulates are incorporated into the base matrix [33]. The production of nanocomposites is currently under exploration and is still at its laboratory scale research level. However, interestingly, when compared to composites with micron-sized reinforcements, nanocomposites exhibit comparable or better mechanical properties with the use of lesser amount of reinforcements [9–12]. Both casting and powder metallurgy (PM) methods can be used to fabricate metal matrix nanocomposites. Historically, PM methods have been developed successfully and commercially used by different manufactures and have also been applied in the production of MMCs for aerospace applications. As compared to casting methods, PM approach has shown its advantage to produce uniform microstructures leading to develop high-performance composite materials [34].

At present, the development of metal matrix composites with light metal matrices are gaining increasing attention due to their enhanced properties coupled with weight savings. These unique properties make them attractive for automotive and aircraft industries in which the weight reduction is the critical factor. So far, extensive studies have been done for the production of aluminum matrix composites and now these are being manufactured commercially for numerous industrial applications. The development of economical aluminum nanocomposites using cost-effective fabrication techniques will serve the requirement of the development of light-weight structural materials well suited to industrial and commercial applications. The main objective of our study was to fabricate high-performance aluminum metal matrix composites through cost-effective processing technique based on PM route incorporating microwave sintering method. A comparison of the microstructural, mechanical, and thermal properties is presented to elucidate the usefulness of the manufactured composite materials.

### 3. Fabrication of Al metal matrix composites

In the current book chapter, the presented composite materials were synthesized through the powder metallurgy method of mixing the matrix (pure aluminum) and reinforcements (SiC,  $\text{Si}_3\text{N}_4$ , and  $\text{Al}_2\text{O}_3$ ). **Figure 3** presents the schematic flow chart of the experimental design. To produce Al-SiC nanocomposites, nano-sized SiC powder (1.5 vol.%) was added to pure Al.



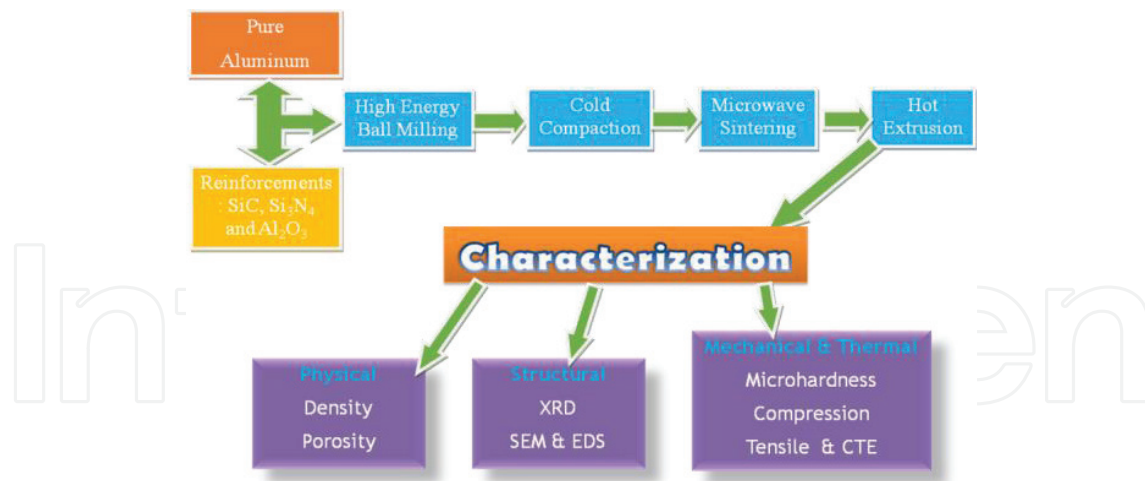


**Figure 3.** Schematic flow chart of the experimental design.

The blending of the mixture was carried out at room temperature using a Retsch PM400 planetary ball mill for 2 h with the milling speed of 200 rpm in order to get a homogeneous particle distribution. No balls were used in this stage. The ball milled powders were cold compacted using a uniaxial pressure of 50 tons into billets (40 mm length with 35 mm diameter). The sintering of the compacted cylindrical billets was carried out at 550°C using an innovative microwave sintering process [35], just below the melting temperature of Al. The other metal matrix composites (Al-1.5 vol.% Si<sub>3</sub>N<sub>4</sub> and Al-15 vol.% Al<sub>2</sub>O<sub>3</sub>) were also prepared in a similar manner.

Prior to hot extrusion, the microwave sintered billets were soaked at 400°C for 1 h and then hot extruded at 350°C and 500 MPa. The extrusion ratio was ~20.25:1 to produce an 8 mm diameter extruded rod, as can be seen in **Figure 4(a)**. After extrusion, these rods were subsequently used for characterization studies.

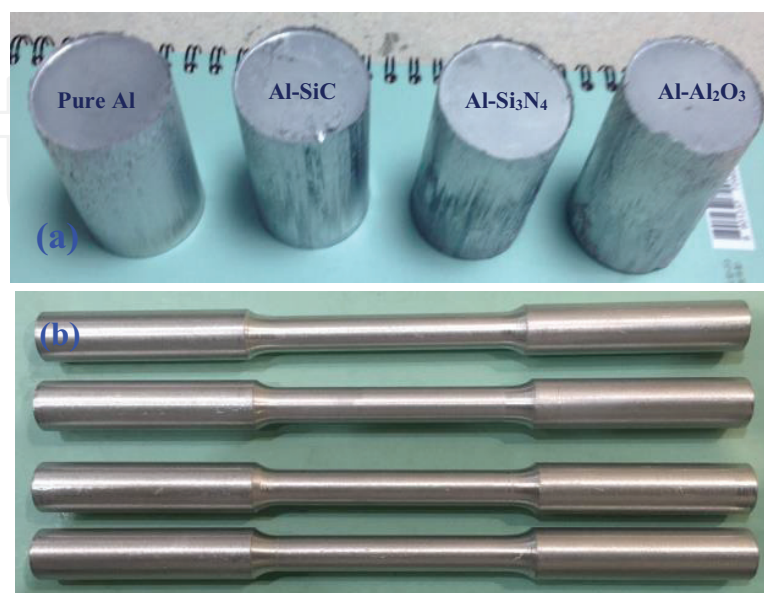


**Figure 4.** The pictures of the produced AMMCs.

The phase identification of the extruded samples was carried out using X-ray powder diffractometer (PANalytical X'pert Pro) based on Cu-K $\alpha$  radiation (1.541 Å) in the  $2\theta$  range of 30–80° at scan rate of 0.2°/min. Individual phases were identified by matching the typical X-ray diffraction (XRD) peaks against JCPDS data. Field emission scanning electron microscopy (SEM) (JEOL JSM-6010 and Hitachi FESEM-S4300) with energy dispersion spectroscopy (EDS) was used to identify the reinforcement phase and microstructure of the extruded composite samples.

The hardness testing of the pure Al and composite samples was carried out using Vicker's hardness tester with applied load of 100 gf for 15 s as per the ASTM standard E384-08. Compressive testing of the cylindrical specimens was performed at room temperature according to the procedures outlined in ASTM standard E9-89a using Universal testing machine-Lloyd. Tensile testing of the extruded pure Al and its composite samples was done using a universal testing machine-Lloyd according to the ASTM E8/E8M-15a standard at room temperature under the strain rate of  $8.3 \times 10^{-4} \text{ s}^{-1}$ . For tensile tests, round test specimens of 25 mm gauge length and 5 mm gauge diameter (**Figure 4(b)**) were prepared and tested on a fully automated servo-hydraulic mechanical testing machine, MTS-810. For every composition, three samples were tested to check repeatable values. The fractured surfaces of the selected compression and tensile specimens were studied by scanning electron microscope (Hitachi FESEM-S4300). Nanoindentation investigation was done using a MFP-3D Nanoidenter (head connected to AFM equipment) system equipped with standard Berkovich diamond indenter tip. The testing was performed at room temperature and the values of hardness (H) and Young's modulus (E) were directly obtained. The presented nanoindentation results are the average of six indentations values. Coefficients of thermal expansion of pure Al and developed composites were determined in the temperature range of 50–350°C using a INSEIS TMA PT 1000LT thermo-mechanical analyzer. A heating rate of 5°C/min was employed at argon flow rate of 0.1 lpm.

## 4. Properties of Al metal matrix composites

### 4.1. X-ray diffraction analysis of AMMCs

The X-ray diffraction (XRD) patterns for the microwave sintered and hot extruded pure Al and Al metal matrix with reinforcement particles SiC, Si<sub>3</sub>N<sub>4</sub>, and Al<sub>2</sub>O<sub>3</sub> are shown in **Figure 5**.

The diffraction peaks of Al, SiC, Si<sub>3</sub>N<sub>4</sub>, and Al<sub>2</sub>O<sub>3</sub> phases can be observed. The sharp peaks representing the presence of Al phase in the XRD patterns. The presence of SiC, Si<sub>3</sub>N<sub>4</sub>, and Al<sub>2</sub>O<sub>3</sub> particles is indicated by minor peaks. The peaks of Al are indexed as (2 2 0), (3 1 1), (1 1 1), (2 0 0), and (2 2 2), whereas SiC peaks are as (1 1 1), (2 0 0); Si<sub>3</sub>N<sub>4</sub> peak as (1 2 0); and Al<sub>2</sub>O<sub>3</sub> peaks are as (0 1 2), (1 0 4), (1 1 3), (0 2 4), (1 1 6), (2 1 4), (3 0 0). During the microwave sintering and hot subsequent extrusion process, it is noted that no solid-state reaction took place between the matrix and reinforcement to form any other undesired phases. The XRD results also approve the elemental mapping results, as will be shown later in **Figure 7**, which verifies the fabrication of phase pure different ceramic-reinforced Al-composites.

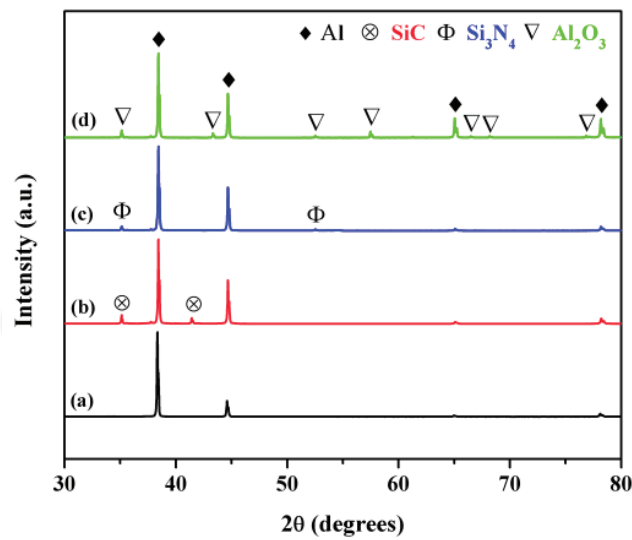


**Figure 5.** XRD patterns for (a) pure Al, (b) Al-SiC, (c) Al-Si<sub>3</sub>N<sub>4</sub>, and (d) Al-Al<sub>2</sub>O<sub>3</sub> composites.

#### 4.2. SEM analysis of AMMCs

Scanning electron microscopy (SEM) was used in order to analyze the morphology and microstructure of developed composites containing different reinforcements. **Figure 6** shows the SEM micrographs of microwave sintered-hot extruded pure Al and Al-X (X = SiC, Si<sub>3</sub>N<sub>4</sub> and Al<sub>2</sub>O<sub>3</sub>) composites.

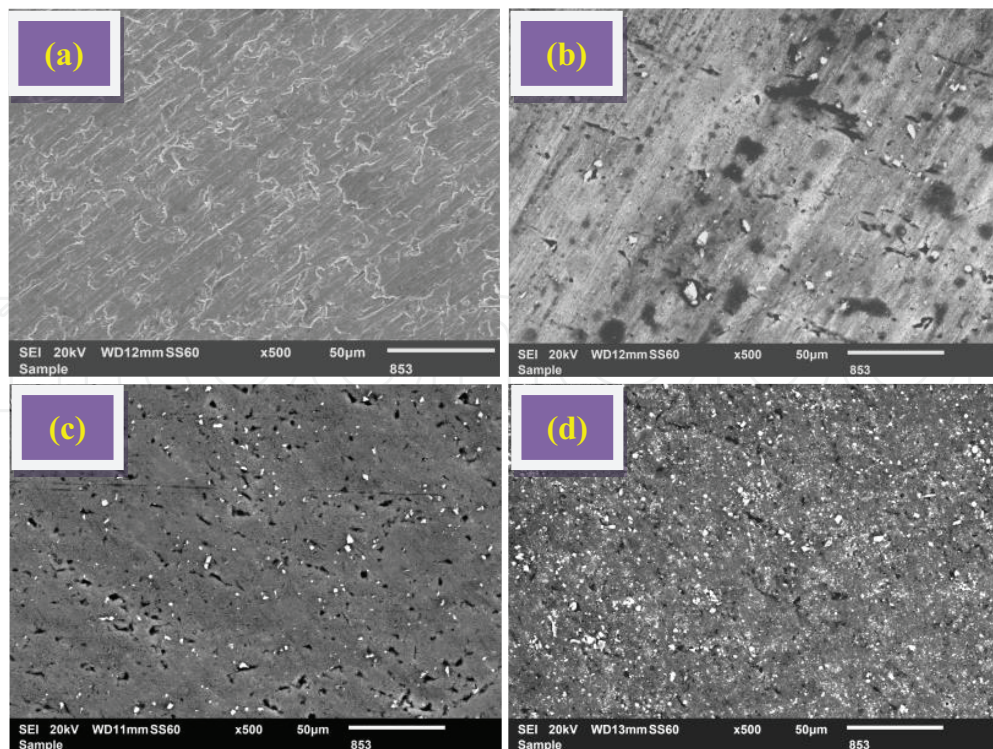


**Figure 6.** FESEM images for (a) pure Al, (b) Al-SiC, (c) Al-Si<sub>3</sub>N<sub>4</sub>, and (d) Al-Al<sub>2</sub>O<sub>3</sub> composites.



The results revealed a fair uniform distribution of ceramic reinforcement particles in the aluminum matrix. It can be further noted that SEM images show two main phases: the grey matrix is the Al phase while the dispersed phase showing white spots represents the SiC,  $\text{Si}_3\text{N}_4$ , and  $\text{Al}_2\text{O}_3$  particles used as reinforcements. At some spaces, agglomeration of reinforcement particulates has been observed (**Figure 6(d)**) which is due to density differences of reinforcements and the aluminum matrix.

The mechanical properties of Al-MMCs are dependent on the nature and distribution of the reinforcement particles. Homogeneous and intragranular distribution is preferred to attain improved properties, and importantly, the hot extrusion process has led to the desirable distribution. Previous studies have reported that agglomeration of reinforcement particles in Al matrix has resulted in the degradation of mechanical properties, as reinforcement clustering along with voids act as pre-existing cracks, limiting the stress transfer from soft matrix to hard phase particles during the deformation process [36, 37].

In our developed Al-composites, the agglomeration of reinforcements is observed only in a few locations, confirming a uniform reinforcement distribution in the Al-X composites. This near-uniform distribution of reinforcement promotes even heating (by absorbing the microwave energy) through the compact during sintering and demonstrates the effectiveness of using powder metallurgy and microwave sintering for the synthesis of Al-based composites [38]. Hence, the SEM results show that microwave sintering followed by hot extrusion process has an appropriate potential for manufacturing the ceramic particle-reinforced metal matrix composites.

#### 4.3. EDS analysis of AMMCs

The energy dispersive spectroscopy (EDS) technique was used to study the composition and elemental distribution of phases present in the Al-based composites.

**Figure 7(a–c)** shows the EDS mapping analysis of microwave-hot extruded pure Al and Al-X ( $X = \text{SiC}$ ,  $\text{Si}_3\text{N}_4$ , and  $\text{Al}_2\text{O}_3$ ) composites. The elemental distribution of phases such as aluminum (matrix) and ceramic particles (reinforcements) is clearly observable. Furthermore, the reinforcing elements are uniformly dispersed all over the aluminum matrix. This confirms the appropriate mixing of ceramic reinforcement particles with the aluminum matrix. **Figure 7(a)** represents the corresponding Al, Si, and composition maps of the Al-SiC composite. **Figure 7(b)** shows the corresponding Al, Si, and N composition maps of the Al- $\text{Si}_3\text{N}_4$  composite. **Figure 7(c)** shows the EDS Al and O composition maps of the Al- $\text{Al}_2\text{O}_3$  composite. Further, the elemental distribution map evidently reveals the uniform distribution of ceramic reinforcement particles in Al matrix and confirms the presence of aluminum, SiC,  $\text{Si}_3\text{N}_4$ , and  $\text{Al}_2\text{O}_3$  phases in respective composition.

#### 4.4. Mechanical properties of AMMCs

The amount and size of reinforcement particles, type of processing technique, and the matrix/particle integrity greatly influence the mechanical properties of an Al-based composite. A strong matrix/particle interface integrity was obtained in this study. Therefore, the volume

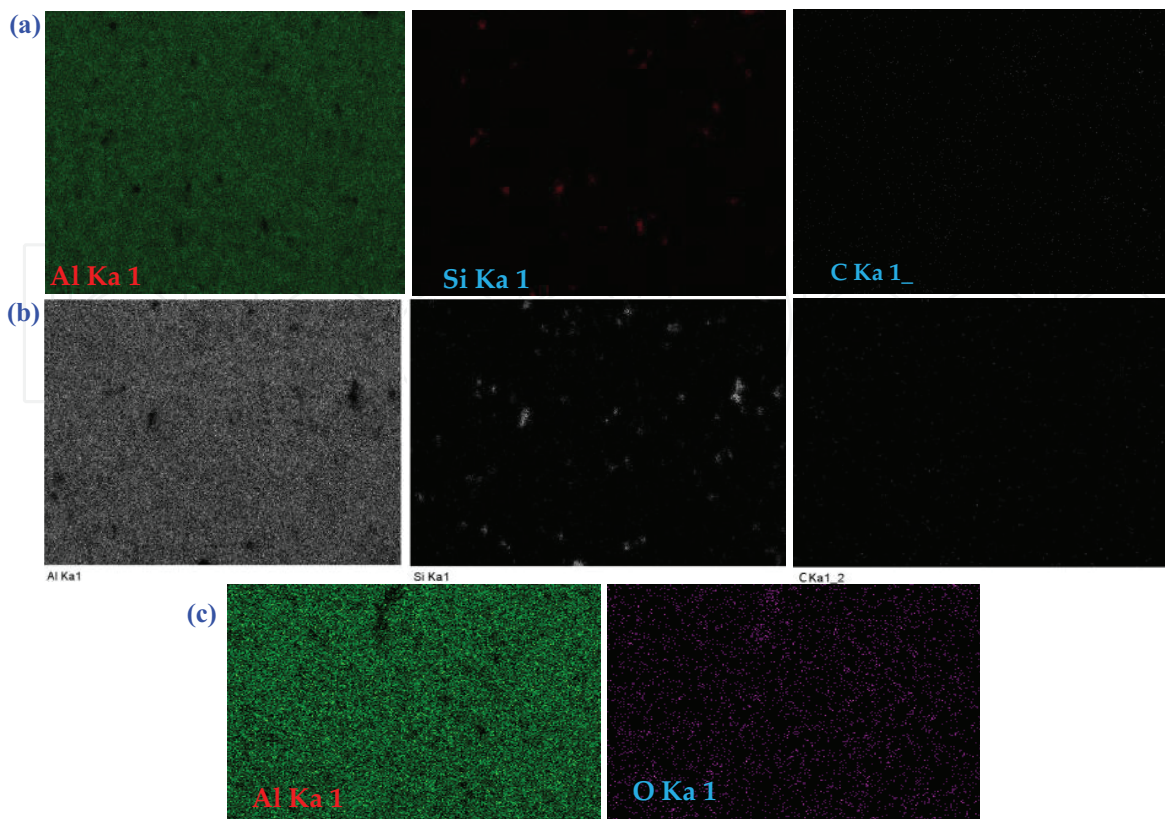


**Figure 7.** EDS maps of AMMCs reinforced with (a) SiC, (b)  $\text{Si}_3\text{N}_4$ , and (c)  $\text{Al}_2\text{O}_3$ .

fraction of the reinforced ceramic particles and the effect of hot extrusion, as a secondary processing, play an active role in improving the mechanical properties of the composites.

#### 4.4.1. Microhardness studies of AMMCs

The microhardness is a very useful important property that reflects the strength of the material. Generally, several factors would affect the microhardness of the composites, such as particle shape, size, amount, distribution, density of reinforcement, and method of preparation [39].

**Figure 8** shows the microhardness of the microwave sintered-extruded pure Al, SiC,  $\text{Si}_3\text{N}_4$ , and  $\text{Al}_2\text{O}_3$  reinforced composite. The hardness of the Al-X (X = SiC,  $\text{Si}_3\text{N}_4$ , and  $\text{Al}_2\text{O}_3$ ) composites is higher than the pure aluminum. The Al-1.5 vol.% SiC, Al-1.5 vol.%  $\text{Si}_3\text{N}_4$ , and Al-15 vol.%  $\text{Al}_2\text{O}_3$  composites exhibit a hardness of  $82 \pm 4$ ,  $101 \pm 3$ , and  $92 \pm 5$  Hv, respectively; these values are comparatively higher than the unreinforced aluminum. However, a remarkable enhancement to  $101 \pm 3$  is observed for  $\text{Si}_3\text{N}_4$  reinforced Al composite. The increase in the microhardness of AMMCs indicates that the ceramic particles has a major contribution in the strengthening of Al matrix. This increase in the hardness is because of the contribution of the reduced crystallite size of  $\sim 15$  nm ( $\text{Si}_3\text{N}_4$ ) compared to 35 nm (SiC) in the composite.

The presence of hard ceramic particles can enhance the microhardness of composites according to the rule of mixtures [40].

$$H_c = H_m f_m + H_r f_r \quad (1)$$

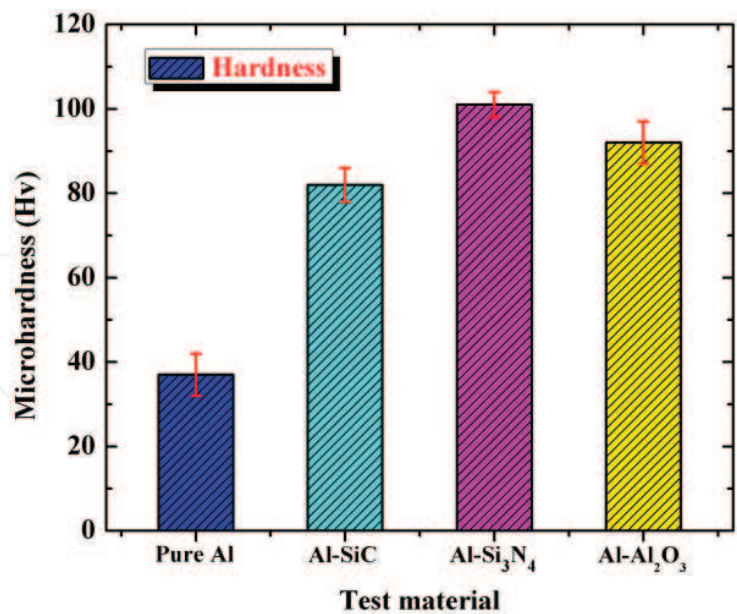


Figure 8. Hardness of aluminum metal matrix composites.

where  $H_c$  represents hardness of the composite,  $H_m$  and  $H_r$  represent hardness of the matrix and the reinforcing particle, respectively, and  $f_m$  and  $f_r$  represent the volume fraction of the matrix and the reinforcing particle, respectively.

The dispersion of hard ceramic reinforcement in the soft aluminum matrix results in strengthening of the structure. Referring to Hall-Petch relationship, the mechanical properties of the metallic materials are affected by the grain size. The grain size of metal matrix composites is smaller than that of the aluminum matrix because of grain refinement of reinforced ceramic particles. The fine grains enhance the hardness of the resulting structure. In addition, the difference in thermal shrinkage between the aluminum matrix and the ceramic particles produces quench hardening effect [41]. The presence of hard ceramic particles also improves the mechanical properties due to dispersion hardening of soft aluminum matrix. In fact, the presence of hard particles impedes the motion dislocation and thus improves the mechanical properties [42].

4.4.2. Compressive studies of AMMCs

The true stress-strain curves of the microwave sintered-hot extruded pure Al and Al-X ( $X = \text{SiC}$ ,  $\text{Si}_3\text{N}_4$ , and  $\text{Al}_2\text{O}_3$ ) composites under compression loading at room temperature are shown in **Figure 9**. The average compressive yield strength (CYS) and ultimate compressive strength (UCS) values of the extruded composites are listed in **Table 1**.

A significant improvement in the strength of Al-X composites are observed compared to pure aluminum. The compression strength of pure Al was increased by adding various ceramic reinforcement particles. The Al-1.5 vol.% SiC composite showed the compressive yield strength (0.2% CYS) and the ultimate compressive strength (UCS) of ~114 and ~392 MPa, respectively, the incremental increase is ~26 and ~72%, respectively, compared to pure Al. In the case of Al-1.5 vol.%  $\text{Si}_3\text{N}_4$  composite, the (CYS) (UCS) were ~142 and ~412 MPa, respectively, showing

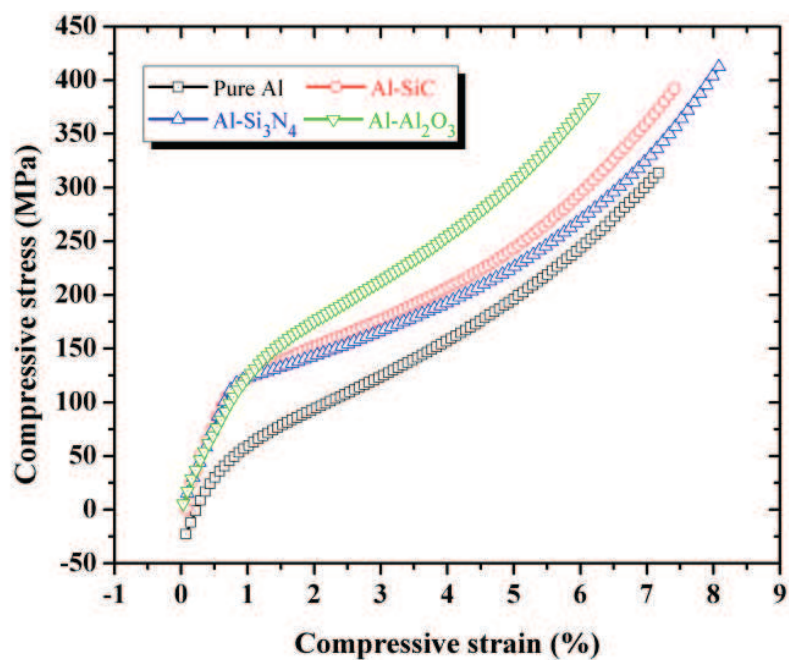


**Figure 9.** Compressive stress-strain curves of aluminum metal matrix composites.

an increase of ~31 and ~115%, respectively, compared to pure Al. The addition of micron-sized alumina particles, Al-15 vol.%  $\text{Al}_2\text{O}_3$  composite exhibited (UCS) ~136 MPa and (CYS) 338 MPa which is ~24 and ~106%, respectively, higher than that of pure Al. The Al-X ( $X = \text{SiC}$ ,  $\text{Si}_3\text{N}_4$  and  $\text{Al}_2\text{O}_3$ ) composites exhibited higher compressive failure strain values when compared to that of pure Al (~7.1%).

This significant improvement in compression strength properties of the extruded Al-X ( $X = \text{SiC}$ ,  $\text{Si}_3\text{N}_4$  and  $\text{Al}_2\text{O}_3$ ) composites compared to the pure Al can be ascribed to the coupled effects of (i) uniform distribution of reinforcing particles in the matrix and (ii) enhanced dislocation density [39]. For a clearer comparison, we have noticed that the compressive properties of the microwave sintered-hot extruded Al-X ( $X = \text{SiC}$ ,  $\text{Si}_3\text{N}_4$  and  $\text{Al}_2\text{O}_3$ ) composites are interestingly superior to that of conventional sintered AMMCs [43–47].

Materials	Nanoindentation data		Compressive properties			Tensile properties		
	Hardness (GPa)	Young's modulus (GPa)	CYS (MPa)	UCS (MPa)	Failure Strain (%)	TYS (MPa)	UTS (MPa)	Elongation (%)
Pure Al	$5.15 \pm 0.3$	$73 \pm 5$	$70 \pm 3$	$313 \pm 5$	7.17	$105 \pm 2$	$119 \pm 4$	$13.6 \pm 0.3$
Al-1.5 vol.% SiC	$9.60 \pm 0.6$	$81 \pm 6$	$114 \pm 7$	$392 \pm 6$	7.48	$158 \pm 9$	$178 \pm 6$	$7.3 \pm 0.9$
Al-1.5 vol.% $\text{Si}_3\text{N}_4$	$16.34 \pm 0.4$	$94 \pm 2$	$142 \pm 6$	$412 \pm 3$	8.07	$165 \pm 5$	$191 \pm 5$	$8.2 \pm 0.4$
Al-15 vol.% $\text{Al}_2\text{O}_3$	$24.56 \pm 0.8$	$106 \pm 9$	$136 \pm 5$	$388 \pm 8$	6.19	$139 \pm 8$	$154 \pm 6$	$7.2 \pm 0.7$

**Table 1.** Mechanical properties of aluminum metal matrix composites.



4.4.3. Tensile studies of AMMCs

The representative tensile stress-strain curves for microwave sintered-hot extruded pure Al and Al-X (X = SiC, Si<sub>3</sub>N<sub>4</sub>, and Al<sub>2</sub>O<sub>3</sub>) composites at room temperature are shown in **Figure 10**. The variations in the tensile strength, yield strength, and ductility with reinforcement addition are listed in **Table 1**. It can be observed that all composites exhibited higher tensile strengths in comparison to that of pure Al. However, the elongation of the composites decreases as compared to pure Al. The calculated decrease is in elongation compared to microwave sintered-extruded pure Al is 46, 39, and 47% for Al-1.5 vol.% SiC, Al-1.5 vol.% Si<sub>3</sub>N<sub>4</sub>, and Al-15 vol.% Al<sub>2</sub>O<sub>3</sub> composites, respectively.

Moreover, **Table 1** also shows that the tensile properties of the Al-1.5 vol.% Si<sub>3</sub>N<sub>4</sub> composites are comparable/superior to that of the SiC and Al<sub>2</sub>O<sub>3</sub> reinforced Al composites. This can be endorsed to the reduced size of the reinforcing particles employed [37]. Like compressive properties, the tensile properties of microwave sintered-extruded Al-X (X = SiC, Si<sub>3</sub>N<sub>4</sub>, and Al<sub>2</sub>O<sub>3</sub>) composites are found superior to the conventional sintered AMMCs [31–35].

To understand the strengthening effects of ceramic reinforcement particles on the hardness, compression, and tensile properties of composites, such as UTS and YS, it is favorable to discuss the strengthening mechanism in detail. In the present study, strengthening occurs due to following mechanisms: (i) active load transfer from the matrix to the reinforcement, (ii) Orowan strengthening, and (iii) generation of internal thermal stresses because of the difference in the coefficient of thermal expansion (CTE) between the reinforcement particles and matrix phase.

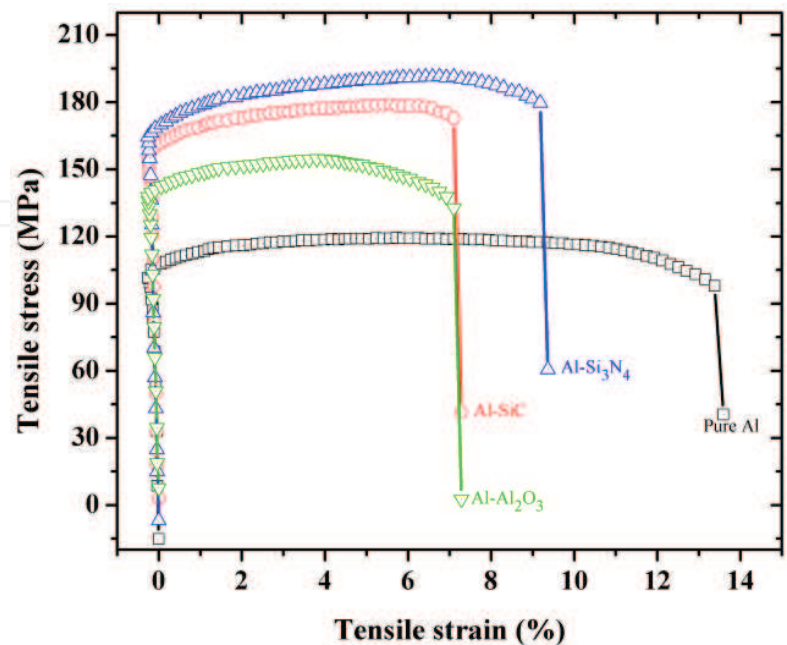


**Figure 10.** Tensile stress-strain curves of aluminum metal matrix composites.

The efficient load transfer ( $\sigma_{load}$ ) between the ductile matrix and the hard ceramic reinforcement particles during tensile testing occurs, particularly when there is a good interfacial contact between the matrix and the reinforcement and is represented as following [48–50]:

$$\sigma_{load} = 0.5 V_f \sigma_{YM} \quad (2)$$

where  $V_f$  is the volume fraction of ceramic reinforcement particles and  $\sigma_{YM}$  is the matrix yield stress.

The interaction between the dislocations and the reinforcement particles enhances the strength of the composite materials in agreement with the Orowan mechanism. Due to the existence of dispersed reinforcement particles in the matrix, dislocation loops are formed when dislocations interact with the reinforcing particles.  $\sigma_{Orowan}$  can be calculated as [51]:

$$\sigma_{Orowan} = \frac{0.13Gb}{\lambda} \ln \frac{r}{b} \quad (3)$$

where  $G$  is the shear modulus of matrix,  $b$  is the Burgers vector,  $\lambda$  is the inter-particle spacing, and  $r$  is the particle radius.

The difference in the CTE values of the reinforcement particles and the metal matrix produces geometrically necessary dislocations and thermally induced residual stresses. The thermal stresses at the particles and matrix interface make the plastic deformation more tough which, hence, enhances the level of hardness and flow stress. The mismatch strain effect due to the difference between the CTE values of particles and that of the matrix is given by [38]:

$$\Delta \sigma_{CTE} = \sqrt{3} \beta G_m b \sqrt{\frac{24 V_f \Delta \alpha \Delta T}{(1 - V_f) b r_p}} \quad (4)$$

where  $b$  is the strengthening coefficient,  $\Delta \alpha$  is the difference between CTE of matrix and reinforcement, and  $\Delta T$  is the difference between the test and process temperature.

#### 4.4.4. Fractography of AMMCs

Some selected compression and tensile tested fractured surfaces were studied using SEM in order to understand the type of fracture and nature of the bonding between the reinforcing particles and Al of the microwave sintered-extruded Al-X ( $X = \text{SiC}, \text{Si}_3\text{N}_4, \text{Al}_2\text{O}_3$ ) composites.

The fracture morphology of microwave sintered-extruded pure Al and Al-X ( $X = \text{SiC}, \text{Si}_3\text{N}_4, \text{Al}_2\text{O}_3$ ) composites during compression test are shown in **Figure 11(a–d)**. The fracture surfaces are comparatively smooth and the formation of shear band can barely be seen in the fractured samples. The fractured compressive samples reveal a crack at  $45^\circ$  to the test axis. **Figure 11(a–d)** shows a typical shear mode fracture in pure Al and Al-X (composites reinforced with various ceramic particles). It approves that the compressive deformation of the Al composites is expressly indifferent. This is due to heterogeneous deformation and work hardening behavior [52]. In contrast, mixed fracture surface and the shear band formation is found in Al- $\text{Al}_2\text{O}_3$

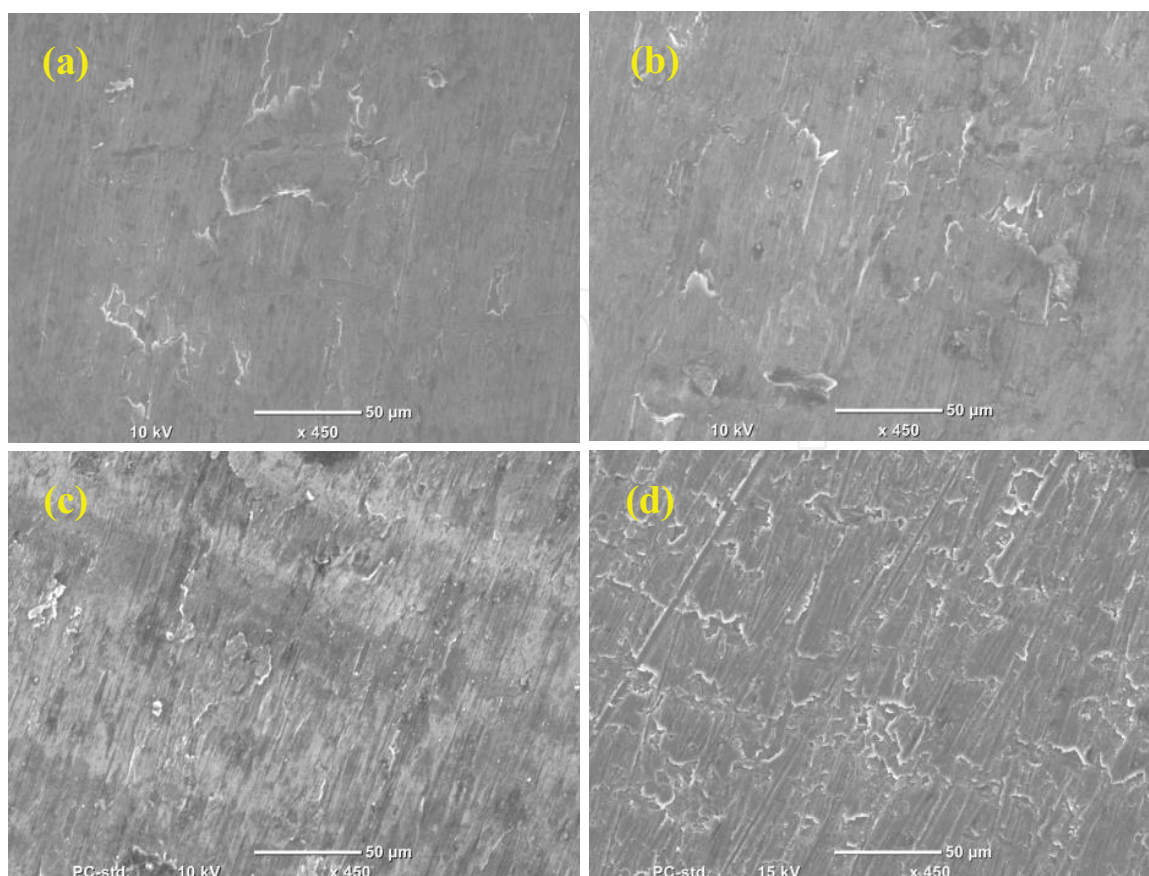


**Figure 11.** SEM micrographs of the compression fracture surfaces of (a) pure aluminum, (b) Al-SiC, (c) Al-Si<sub>3</sub>N<sub>4</sub>, and (d) Al-Al<sub>2</sub>O<sub>3</sub>.

composite (**Figure 11(d)**). The plastic deformation in the composites was inhibited due to the dispersion of second phases. This led to the significant reduction in compressive failure strain in the composite (see **Table 1**).

Fracture morphology of pure Al and its composites during tensile testing are presented in **Figure 12**. The examination of fractured surfaces reveals the formation of similar ductile fracture in all composites. For Al-SiC composites, the fractured surfaces shows dimple-like fracture which can be related to the observed failure strain of more than 7% (see **Table 1**). The presence of SiC particles in the dimple cores and walls suggests that the fractured particles and agglomerates are potential stress concentration sites and susceptible to void formation. Al-Si<sub>3</sub>N<sub>4</sub> composites showed the strongest bonding as revealed by the good matrix/reinforcement performance. For Al-Al<sub>2</sub>O<sub>3</sub> composites, it can be seen that ductile failure occurs in the matrix, whereas brittle, cleavage-type failure is seen to be predominant in regions where Al<sub>2</sub>O<sub>3</sub> particles are present. Large number of dimples with tear ridges is also seen in the Al-Al<sub>2</sub>O<sub>3</sub> composite.

#### 4.4.5. Coefficient of thermal expansion of AMMCs

The variation of CTE of microwave sintered-extruded pure Al and Al-X composites (X = SiC, Si<sub>3</sub>N<sub>4</sub>, Al<sub>2</sub>O<sub>3</sub>) is shown in **Figure 13**. It can be observed that the CTE values decrease with reinforced ceramic particles. It is in accordance with the theory that the thermal expansion



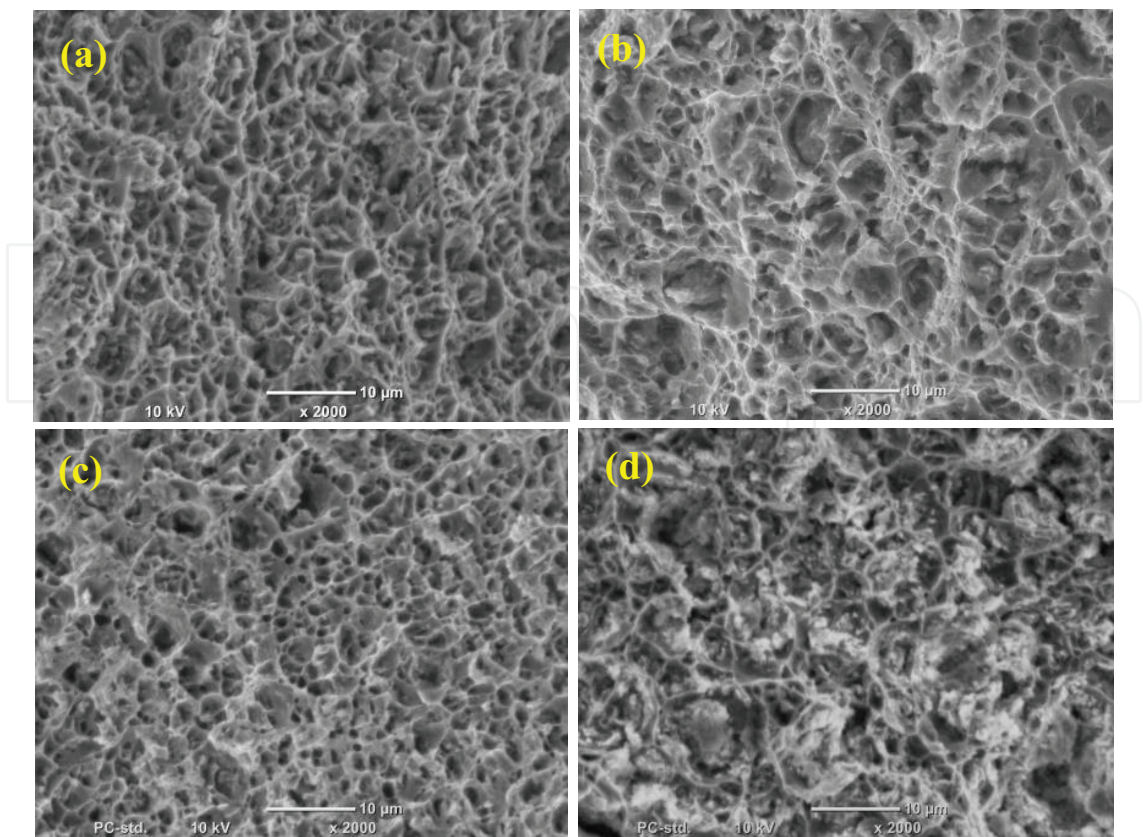


**Figure 12.** SEM micrographs of the tensile fracture surfaces of (a) pure aluminum, (b)Al-SiC, (c) Al-Si<sub>3</sub>N<sub>4</sub>, and (d) Al-Al<sub>2</sub>O<sub>3</sub>.

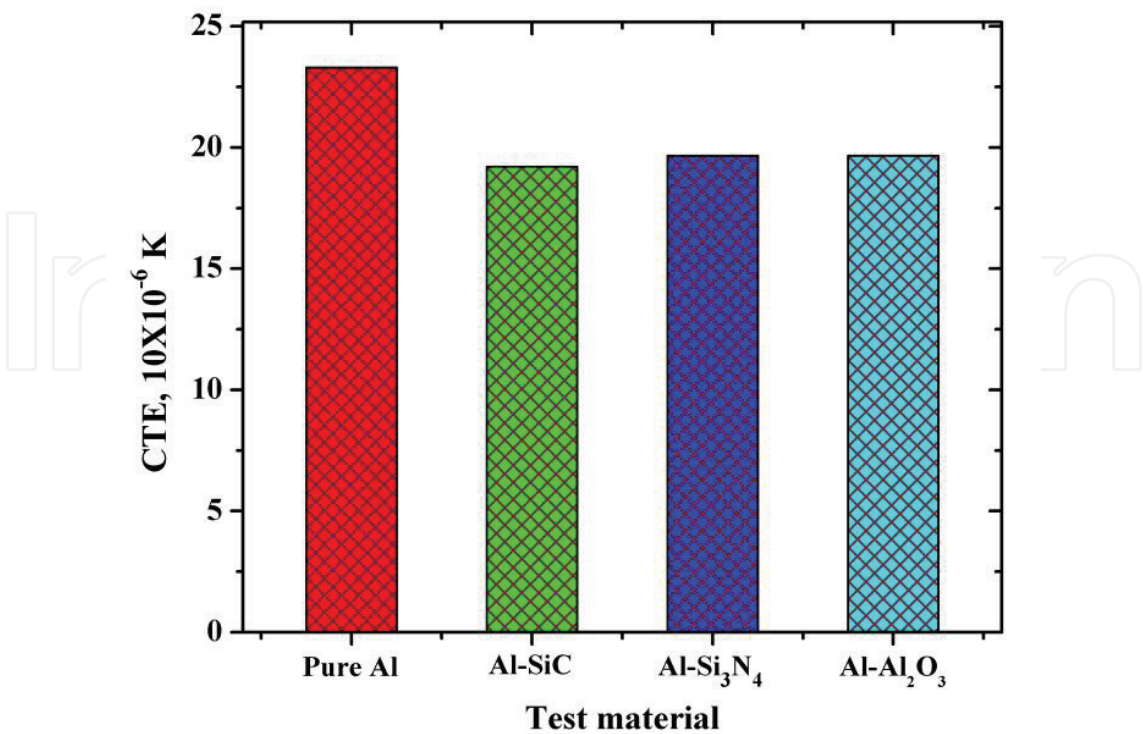


**Figure 13.** CTE of the aluminum metal matrix composites.



of the composites is governed by the competing interactions of expansion of Al matrix and the constraint of ceramic particles through their interfaces [52]. The CTE of pure Al was measured to be  $23.31 \times 10^{-6}/\text{K}$  which is in close agreement with the theoretical CTE of aluminum ( $24 \times 10^{-6}/\text{K}$ ). The addition of nano-sized 1.5 vol.% SiC, nano-sized 1.5 vol.%  $\text{Si}_3\text{N}_4$ , and micron-sized 15 vol.%  $\text{Al}_2\text{O}_3$  particles to Al reduced the CTE value to  $\sim 19.20 \times 10^{-6}/\text{K}$ ,  $19.43 \times 10^{-6}/\text{K}$ , and  $19.66 \times 10^{-6}/\text{K}$  which are  $\sim 17.63$ ,  $\sim 16.66$ , and  $\sim 15.65\%$  reduction when compared to pure Al. This considerable decrease in CTE values may be due to the high thermal stability of SiC,  $\text{Si}_3\text{N}_4$ , and  $\text{Al}_2\text{O}_3$  reinforcement particles having theoretical CTE of  $4.3 \times 10^{-6}/\text{K}$  [53],  $3.3 \times 10^{-6}/\text{K}$  [54],  $7.4 \times 10^{-6}/\text{K}$  [53], respectively. The linear decrease in CTE values with the addition of ceramic particles can be attributed to: (i) the lower CTE values of ceramic (SiC,  $\text{Si}_3\text{N}_4$ , and  $\text{Al}_2\text{O}_3$ ) particles reinforcements as compared to that of the pure Al matrix; and (ii) uniform distribution of the ceramic reinforcements in the matrix.

The compatible CTE of Al-X composites ( $X = \text{SiC}$ ,  $\text{Si}_3\text{N}_4$ ,  $\text{Al}_2\text{O}_3$ ) and high dimensional stability makes these microwave sintered-extruded composite very competitive for application in aerospace and automotive industry.

## 5. Conclusions

Al-X ( $X = \text{SiC}$ ,  $\text{Si}_3\text{N}_4$ , and  $\text{Al}_2\text{O}_3$ ) composites were successfully synthesized through microwave-assisted powder metallurgy route coupled with hot extrusion process. Various ceramic reinforcement particles were added into Al matrix, and their effect on structural, mechanical, and thermal properties has led to the following conclusions.

- XRD patterns of Al-X ( $X = \text{SiC}$ ,  $\text{Si}_3\text{N}_4$ ,  $\text{Al}_2\text{O}_3$ ) composites indicate that the main components of the synthesized composites are Al, SiC,  $\text{Si}_3\text{N}_4$ , and  $\text{Al}_2\text{O}_3$ .
- Homogeneous reinforcement particles distribution was found in microwave sintered-extruded Al-X ( $X = \text{SiC}$ ,  $\text{Si}_3\text{N}_4$ ,  $\text{Al}_2\text{O}_3$ ) composites. This shows that the microwave sintering coupled with extrusion process has an appropriate potential to process high-performance particle-reinforced metal matrix composites.
- A comparison of mechanical properties (hardness, strength) indicates that microwave sintered-extruded Al-X ( $X = \text{SiC}$ ,  $\text{Si}_3\text{N}_4$ ,  $\text{Al}_2\text{O}_3$ ) composites have superior properties compared to microwave sintered-extruded pure Al. The improvement in mechanical properties can be attributed to (i) active load transfer from the matrix to the reinforcement, (ii) Orowan strengthening, and (iii) generation of internal thermal stresses because of the difference in the coefficient of thermal expansion (CTE) between the reinforcement particles and matrix phase.
- The produced Al-X ( $X = \text{SiC}$ ,  $\text{Si}_3\text{N}_4$ ,  $\text{Al}_2\text{O}_3$ ) composites have low ductility compared to pure Al due to low inherent ductility of ceramic particles used as reinforcement.
- The fractography results indicate that under compressive loading, the Al-X ( $X = \text{SiC}$ ,  $\text{Si}_3\text{N}_4$ ,  $\text{Al}_2\text{O}_3$ ) composites show the presence of shear bands which confirms the brittle mode of fracture. However, under tensile loading, the dimple formation was noticed on the fractured surfaces endorsing ductile mode of fracture.

- Coefficient of thermal expansion values decreases with the addition of ceramic-reinforced particles into Al matrix confirming high-dimensional stability of microwave sintered-extruded Al-X (X = SiC, Si<sub>3</sub>N<sub>4</sub>, Al<sub>2</sub>O<sub>3</sub>) composites making them suitable for automotive and many other related applications.

## Acknowledgements

This chapter was made possible by NPRP Grant 7-159-2-076 from Qatar National Research Fund (a member of the Qatar Foundation). Statements made herein are solely the responsibility of the authors.

## Author details

Penchal Reddy Matli<sup>1</sup>, Rana Abdul Shakoor<sup>1\*</sup> and Adel Mohamed Amer Mohamed<sup>2</sup>

\*Address all correspondence to: [shakoor@qu.edu.qa](mailto:shakoor@qu.edu.qa)

<sup>1</sup> Center for Advanced Materials, Qatar University, Doha, Qatar

<sup>2</sup> Department of Metallurgical and Materials Engineering, Suez University, Suez, Egypt

## References

- [1] Sutton WH. Microwave processing of ceramic materials. American Ceramic Society Bulletin. 1989;**68**:376-386
- [2] Sutton WH. Ceramic transactions microwaves: Theory and applications in materials processing II. Key issues in microwave process technology. 1993;**36**:3-18
- [3] Das S, Mukhopadhyay AK, Datta S, Basu D. Prospects of microwave processing: An overview. Bulletin of Materials Science. 2009;**32**:1-13
- [4] Xie Z, Wang C, Fan X, Huang Y. Microwave processing and properties of Ce-Y-ZrO<sub>2</sub> ceramics with 2.45 GHz irradiation. Materials Letters. 1999;**38**:190-196
- [5] Agrawal DK. Microwave processing of ceramics: A review. Current Opinion in Solid State Materials Science. 1998;**3**:480-486
- [6] Penchal Reddy M, Madhuri W, Ramamanohar Reddy N, Siva Kumar KV, Murthy VRK, Ramakrishna Reddy R. Magnetic properties of Ni-Zn ferrites prepared by microwave sintering method. Journal of Electroceramics. 2012;**28**:1-9
- [7] Hao HS, Xu LH, Huang Y, Zhang XM, Xie ZP. Kinetics mechanism of microwave sintering in ceramic materials. Science in China Series E: Technological Sciences. 2009;**52**:2727-2731

- [8] Oghbaei M, Mirzaee O. Microwave versus conventional sintering: A review of fundamentals, advantages and applications. *Journal of Alloys and Compounds*. 2010;**494**:175-189
- [9] Roy R, Agrawal D, Cheng J, Gedevanishvili S. Full sintering of powdered-metal bodies in a microwave field. *Nature*. 1999;**399**:668-670
- [10] Lianxi H, Erde W. Fabrication and mechanical properties of SiCw/ZK51A magnesium matrix composite by two-step squeeze casting. *Materials Science and Engineering A*. 2000;**278**:267-271
- [11] Jia DC. Influence of SiC particulate size on the microstructural evolution and mechanical properties of Al-6Ti-6Nb matrix composites. *Materials Science and Engineering A*. 2000;**289**:83-90
- [12] Tang F, Hagiwara M, Schoenung JM. Formation of coarse-grained inter-particle regions during hot isostatic pressing of nanocrystalline powder. *Scripta Materialia*. 2005;**53**: 619-624
- [13] Jenkins I, Wood J. *Powder Metallurgy: An Overview*. London: Institute of Metals; 1991
- [14] Gupta M, Wong WLE. *Microwaves and Metals*. Singapore: John Wiley & Sons Pte. Ltd.; 2007
- [15] Penchal Reddy M, Ubaid F, Shakoor A, Mohamed AMA, Gupta M. Microwave rapid sintering of Al-metal matrix composites: A review on the effect of reinforcements, microstructure and mechanical properties. *Metals*. 2016;**6**:1-19
- [16] Rajkumar K, Aravindan S. Microwave sintering of copper graphite composites. *Journal of Materials Processing Technology*. 2009;**209**:5601-5605
- [17] Leonelli C, Veronesi P, Denti L, Gatto A, Iuliano L. Microwave assisted sintering of green metal parts. *Journal of Materials Processing Technology*. 2008;**205**:489-496
- [18] Binner J, Annapoorani K, Paul A, Santacruz I, Vaidhyanathan B. Dense nanostructured zirconia by two stage conventional/hybrid microwave sintering. *Journal of the European Ceramic Society*. 2008;**28**:973-977
- [19] Menezes RR, Souto PM, Kiminami RHGA. In: Lakshmanan A, editor. *Sintering of Ceramics—New Emerging Techniques Microwave Fast Sintering of Ceramic Materials*. Croatia: InTech; 2012. pp. 3-26
- [20] Madhuri W, Penchal Reddy M, Ramamanohar Reddy N, Siva Kumar KV, Murthy VRK. Comparison of initial permeability of MgCuZn ferrites sintered by both conventional and microwave methods. *Journal of Physics D: Applied Physics*. 2009;**42**:165007
- [21] Bykov Yu V, Rybakov KI, Semenov VE. High-temperature microwave processing of materials. *Journal of Physics D: Applied Physics*. 2001;**34**:R55-R75
- [22] Agrawal D. Microwave sintering of ceramics, composites, metals, and transparent materials. *Journal of Materials Education*. 1999;**19**:49-58

- [23] Agrawal DK, Papworth AJ, Cheng J, Jain H, Williams DB. Microstructural examination by TEM of WC/Co composites prepared by conventional and microwave processes. Powder metallurgical high performance materials. Proceedings. 2001;**2**:677-684
- [24] Rodiger K, Dreyer K, Gerdes T, Porada MW. Microwave sintering of hardmetals. International Journal of Refractory Metals & Hard Materials. 1998;**16**:409-416
- [25] Agrawal D, Cheng J, Seegopaul P, Gao L. Grain growth control in microwave sintering of ultrafine WC/Co composite powder compacts. Powder Metallurgy. 2000;**43**:15-16
- [26] Penchal Reddy M, Ubaid F, Shakoor A, Mohamed AMA, Madhuri W. Structural and mechanical properties of microwave sintered Al-Ni<sub>50</sub>Ti<sub>50</sub> composites. Journal of Science Advanced Materials and Devices. 2016;**1**:362-366
- [27] Wong WLE, Gupta M. Simultaneously improving strength and ductility of magnesium using nano-size SiC particulates and microwaves. Advanced Engineering Materials. 2006;**8**:735-739
- [28] Sankaranarayanan S, Shankar VH, Jayalakshmi S, Bau NQ, Gupta M. Development of high performance magnesium composites using Ni<sub>50</sub>Ti<sub>50</sub> metallic glass reinforcement and microwave sintering approach. Journal of Alloys and Compounds. 2015;**627**:192-199
- [29] Mula S, Panigrahi J, Kang PC, Koch CC. Effect of microwave sintering over vacuum and conventional sintering of Cu based nanocomposites. Journal of Alloys and Compounds. 2014;**588**:710-715
- [30] Aigbodion VS, Hassan SB. Effects of silicon carbide reinforcement on microstructure and properties of cast Al-Si-Fe/SiC particulate composites. Materials Science and Engineering A. 2007;**447**:355-360
- [31] Sharifi EM, Karimzadeh F, Enayati MH. Fabrication and evaluation of mechanical and tribological properties of boron carbide reinforced aluminum matrix nanocomposites. Materials and Design. 2011;**323**:263-3271
- [32] Kainer KU. Basic of Metal Matrix Composites. In: Kainer KU, editor. Metal matrix composites: Custom-made materials for automotive and aerospace engineering. Weinheim, Chichester: Wiley-VCH; 2006
- [33] Ye J, He J, Schoenung JM. Cryomilling for the fabrication of a particulate B<sub>4</sub>C reinforced Al nanocomposite: Part I. Effects of process conditions on structure. Metallurgical and Materials Transactions A. 2007;**37**:3099-3109
- [34] Tjong SC. Novel nanoparticle-reinforced metal matrix composites with enhanced mechanical properties. Advanced Engineering Materials. 2007;**9**:639-652
- [35] Gururaj P, Vyasraj M, Ganesh Kumar M, Gupta M. Enhancing the hardness/compression/damping response of magnesium by reinforcing with biocompatible silica nanoparticles. International Journal of Materials Research. 2016;**107**:1091-1099



- [36] Sun C, Song M, Wang Z, He Y. Effect of particle size on the microstructures and mechanical properties of SiC-reinforced pure aluminum composites. *Journal of Materials Engineering and Performance*. 2011;**20**:1606-1612
- [37] Chawla N, Williams JJ, Saha R. Mechanical behavior and microstructure characterization of sinter-forged sic particle reinforced aluminum matrix composites. *Journal of Light Metals*. 2002;**2**(4):215-227
- [38] Wong WLE, Gupta M. Using microwave energy to synthesize light weight/energy saving magnesium based materials: A review. *Technologies*. 2015;**3**:1-18
- [39] Khadem SA, Nategh S, Yoozbashizadeh H. Structural and morphological evaluation of Al-5 vol% SiC nanocomposite powder produced by mechanical milling. *Journal of Alloys and Compounds*. 2011;**509**:2221-2226
- [40] Roy R, Agrawal D, Cheng J, Mathis M. Microwave processing: Triumph of applications-driven science in WC-composites and ferroic titanates. *Ceramics Transactions*. 1997;**80**:3-26
- [41] Dinaharan I, Sathiskumar R, Murugan N. Effect of ceramic particulate type on microstructure and properties of copper matrix composites synthesized by friction stir processing. *Journal of Materials Research and Technology*. 2016;**5**:302-316
- [42] Sug WK, Lee UJ, Han SW, Kim DK, Ogi K. Heat treatment and wear characteristics of Al/SiCp composites fabricated by duplex process. *Composites: Part B*. 2003;**34**:737-745
- [43] Ezatpour HR, P0061rizi MT, Sajjadi, SA. Microstructure and mechanical properties of extruded Al/Al<sub>2</sub>O<sub>3</sub> composites fabricated by stir-casting process. *Transactions of Nonferrous Metals Society of China*. 2013;**23**:1262-1268
- [44] Davis LC, Andres C, Allison JE. Microstructure and strengthening of metal matrix composites. *Materials Science and Engineering A*. 1998;**294**:40-45
- [45] Sharma P, Sharma S, Khanduja D. Production and some properties of Si<sub>3</sub>N<sub>4</sub> reinforced aluminum alloy composites. *Journal of Asian Ceramic Societies*. 2015;**3**:352-359
- [46] Ma ZY, Li YL, Liang Y, Zheng F, Bi J, Tjong SC. Nanometric Si<sub>3</sub>N<sub>4</sub> particulate-reinforced aluminum composite. *Materials Science and Engineering A*. 1996;**219**:229-231
- [47] Zakeri M, Vakili-Ahrari Rudi A. Effect of shaping methods on the mechanical properties of Al-SiC composite. *Materials Research*. 2013;**16**(5):1169-1174
- [48] Zhang Z, Chen DL. Contribution of Orowan strengthening effect in particulate reinforced metal matrix nanocomposites. *Materials Science and Engineering A*. 2008;**483**:148-152
- [49] Zhang Z, Chen DL. Consideration of Orowan strengthening effect in particulate reinforced metal matrix nanocomposites: A model for predicting their yield strength. *Scripta Materialia*. 2006;**54**:1321-1326
- [50] Habibnejad K, Mahmudi R, Poole WJ. Enhanced properties of Mg-based nano composites reinforced with Al<sub>2</sub>O<sub>3</sub> nano-particles. *Materials Science and Engineering A*. 2009;**519**:198-203

- [51] Ashby MF. Proceedings of the second bolton landing conference on oxide dispersion strengthening. New York: Gordon and Breach, Science Publishers Inc.; 1968
- [52] Anggara B, Soegijono SB. Mechanical properties of metal Al/SiC and AlCu/SiC metal matrix composites (MMCs). *KnE Engineering*. 2016;1-5
- [53] Brandes EA, Brook GB, Smithells Metals Reference Book, Butterworth-Heinemann, London, 1998, pp. 5-12
- [54] Qing CG, Shu YW, Kang MA, Hussain M, Tao JL, Hui WUG. Aging and thermal expansion behavior of  $\text{Si}_3\text{N}_4/\text{2024Al}$  composite fabricated by pressure infiltration method. *Transactions of Nonferrous Metals Society of China*. 2011;**211**:262-273

